ChemPubSoc Europe

DOI: 10.1002/chem.201504618

CHEMISTRY A European Journal Full Paper

Metallacycles

Synthesis of Cyclic Vinylidene Complexes and Azavinylidene Complexes by Formal [4+2] Cyclization Reactions

Jinxiang Chen[+], Zi-Ao Huang[+], Zhengyu Lu, Hong Zhang,* and Haiping Xia*[a]

Abstract: Reactions of the hydrido-butenylcarbyne complex $[OsHCl_2(\equiv CC(PPh_3)=CHEt)(PPh_3)_2]BF_4$ (**1**) with nitriles RC≡N (R = 2-cyclopropyl-2-oxopropyl, 3-amino-2-oxobutyl) lead to six-membered cyclic vinylidene complexes **3** and azavinylidene complexes **4**, that is, iso-osmapyridiniums. Treatment of **1** with excess 2-formylbenzonitrile at reflux temperature in $CHCl_3$ in the presence of air produces a fused osmapyridinium **8**, which is first oxidized to the tricyclic iso-osmapyridinium derivative **7**, then to iso-osmapyridinium **9**, which contains a fused naphthalenone fragment. The conversion of iso-osmapyridinium **9** (with a vinylidene segment) to the iso-osmapyridinium compounds **10** and **11** (with azavinylidene segments) was achieved in the presence of a hydrogen halide, such as HCl or HI. The molecular structures of the complexes synthesized were confirmed by X-ray studies. Moreover, the aromatic stabilization energy and nucleus-independent chemical-shift values of the osmapyridiniums and the strain in the iso-osmapyridinium rings were investigated by DFT calculations.

Introduction

In the form of the simplest unsaturated carbene, vinylidenes have been extensively investigated by both experimentalists and theoreticians.[1] After the discovery of the first terminal vinylidene–metal complex in 1972,[2] vinylidene complexes of various metals have been shown to be key intermediates for the catalytic conversions of alkynes[3] and active substrates in a number of stoichiometric reactions.[4] However, the linear geometry of vinylidene–metal structures makes incorporation of the units into small-ring systems particularly difficult. The first reported cyclic vinylidene–metal complexes (**I**, Scheme 1) were prepared by Esteruelas and co-workers in 2004,[5a] and were described as iso-metallabenzenes in the literature. Other examples of iso-metallabenzenes have been synthesized by formal [3+3] cycloaddition reactions.[5b,c] We have recently verified the existence of the first five-membered metallacycles that contain a metal–vinylidene moiety (**III**) and the conversion of these compounds to their analogous six-membered metallacycles (**II**).[6] So far, reported examples of cyclic vinylidene–metal complexes are limited to these three types.

As depicted in Scheme 1, ketimide ligands are unsaturated ligands that contain a C=N double bond, which can be classified into two bonding modes depending on the number of electrons donating to the metal center. In the literature,[7] the most common bonding mode of ketimide ligands is the $2e^-$ type. In contrast, well-characterized complexes of ketimide ligands with the $4e^-$ bonding type (also described as azavinylidene complexes) are much less prevalent, although the synthesis of such species has been demonstrated by using different transition metals.[7,8] Additionally, azavinylidene complexes have been involved as crucial intermediates in the ammoxidation of propene[9] and the catalytic and stoichiometric reduction of nitriles.[10] Similar to the above-mentioned vinylidene complexes, the linear structural feature also hindered the synthesis of cyclic azavinylidene–metal complexes. To the best of our knowledge, there is only one such metallacyclic example that contains an azavinylidene fragment (i.e., Zr=N=C) inside a seven-membered ring.[8d]

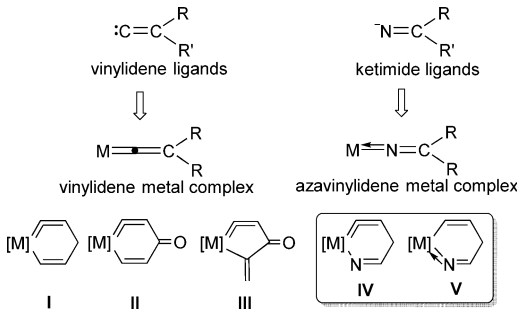

Scheme 1. Vinylidene–metal complexes and azavinylidene–metal complexes.

In 2009, we demonstrated an unprecedented formal [4+2] cycloaddition between the hydrido alkenylcarbyne complex $[OsHCl_2(\equiv CC(PPh_3)=CHPh)(PPh_3)_2]BF_4$ and acetonitrile, which af-

[a] Dr. J. Chen,[+] Z.-A. Huang,[+] Z. Lu, Dr. H. Zhang, Prof. Dr. H. Xia
State Key Laboratory of Physical Chemistry of Solid Surfaces
Collaborative Innovation Center of Chemistry for Energy Materials
and College of Chemistry and Chemical Engineering
Xiamen University, Xiamen, 361005 (P. R. China)
E-mail: zh@xmu.edu.cn
hpxia@xmu.edu.cn

[+] These authors contributed equally to this work.

Supporting information for this article is available on the WWW under http://dx.doi.org/10.1002/chem.201504618.

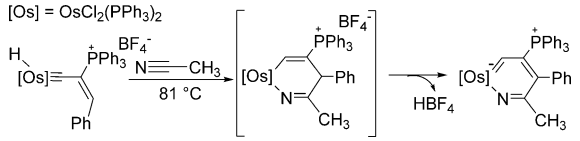

Scheme 2. Proposed osma-azacyclohexadiene intermediate.

forded the first known late-transition-metal-containing metallapyridine complex.[11] As shown in Scheme 2, an osma-azacyclohexadiene complex was proposed as the key reaction intermediate. These results encouraged us to synthesize other interesting heteroatom-containing metallacycles by this novel [4+2] synthetic strategy.

We now report the reactions of hydrido-butenylcarbyne complex $[OsHCl_2(\equiv CC(PPh_3)M{=}CHEt)(PPh_3)_2]BF_4$ (**1**) with nitriles to form rather unusual osmacycles that contain cumulative double bonds. In the course of this research, metallacycles closely related to **IV** and **V** (Scheme 1) have been isolated and characterized, and the strain differences between the isomers have been investigated by DFT calculations. In addition, as an extension to this unique strategy, fused metallacycles with cumulative double bonds have been achieved by using functionalized nitrile starting materials.

Results and Discussion

Reactions of hydrido-butenylcarbyne complex 1 with nitriles

Treatment of hydrido-butenylcarbyne complex **1**[12] with 3-cyclopropyl-3-oxopropanenitrile (2 equiv) in $CHCl_3$ at reflux temperature primarily yielded complex **2a**, along with a small amount of complex **3a** (Scheme 3). When a solution of **1** in $CHCl_3$ was heated at reflux temperature for 12 h **2a** was the dominant product. Compound **2a** was isolated as a yellow solid in 71% yield and was characterized by multinuclear NMR spectroscopy and HRMS.

The structure of the product was further determined by single-crystal X-ray diffraction. The crystallographic details are given in Table 1, and selected bond lengths and angles are given in Table 2. The X-ray structure (Figure 1) clearly shows that complex **2a** contains an essentially planar six-membered

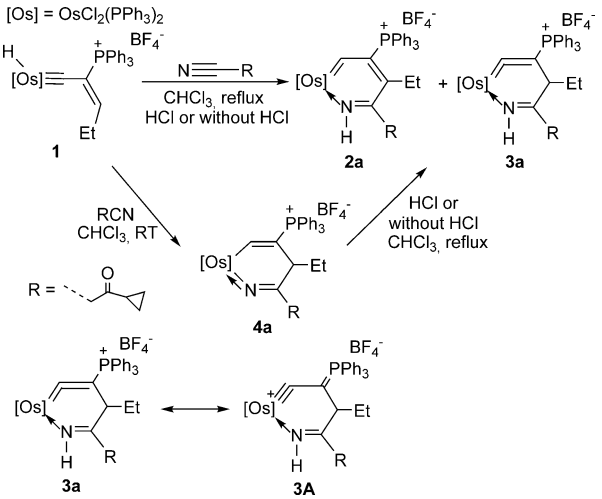

Scheme 3. Reactions of **1** with nitriles.

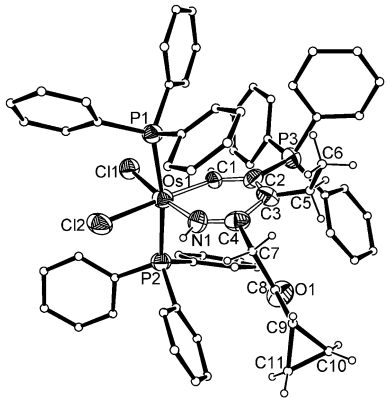

Figure 1. Molecular structure of **2a**. The hydrogen atoms of PPh_3 are omitted for clarity.

metallapyridinium unit. The structural features associated with the metallacycle of **2a** are similar to those of our previously reported osmapyridinium.[11,13] The mean deviation from the least-squares plane through Os1, N1, and C1–C4 is 0.0584 Å, and the sum of the angles of the six-membered ring is 718.2°, which is very close to the ideal value of 720°. The bond distances within the metallacycle all fall within the range typically observed for other metalla-aromatic complexes.[14] The structural data and the planar nature of **2a** indicate a delocalized structure.

It is interesting that complex **3a** was obtained as the major product and was isolated as a yellow solid in 63% yield when the reaction was performed in the presence of excess HCl. Compound **3a** was characterized by NMR spectroscopy and HRMS. The ^{1}H NMR spectra of **3a** displayed only two ring proton signals at $\delta = 3.8$ and 12.4 ppm, which represented the protons on C3 and N1 of the metallacycle, respectively. The ^{13}C NMR spectra displayed the Os=C1 signal at $\delta = 271.3$ ppm and the signals for the remaining carbon atoms of the metallacycle at $\delta = 173.0$ (C4), 122.3 (C2), and 41.3 ppm (C3).

The structure of complex **3a** was also confirmed by X-ray diffraction (Figure 2). Complex **3a** contains an essentially planar six-membered metallacycle, and the sum of the angles in the six-membered ring is 718.8°. The mean deviation from the least-squares plane through Os1, N1, and C1–C4 is 0.0433 Å. The Os1=C1 bond length (1.780(7) Å) is at the low end of the range for typical Os=C=CRR′ bonds (1.762–1.946 Å),[15] which indicates the dominance of the resonance form **3A** (Scheme 3). The Os1–N1 bond length (2.082(6) Å) is within the range of reported values for Os–N single bonds (1.635–2.543 Å).[15] The other C–C and C–N bond lengths in the ring are similar to typical double- or single-bond lengths. The structural data indicate that **3a** is the first iso-metallapyridinium with form **IV** (Scheme 1), which is closely related to the iso-metallabenzenes. It is worth noting that the Os1-C1-C2 angle (150.5(6)°) deviates considerably from linearity and is

Table 1. Crystal data and structure refinement for **2a**, **3a**, **4a**, **4b**, and **5**.

	2a·0.5CH_2Cl_2	**3a**·2CH_2ClCH_2Cl	**4a**·2CH_2Cl_2	**4b**·CH_2ClCH_2Cl	**5**·2.5CH_2Cl_2
formula	$C_{65}H_{59}BCl_2F_4NOOsP_3$ ·0.5CH_2Cl_2	$C_{65}H_{59}BCl_2F_4NOOsP_3$ ·2CH_2ClCH_2Cl	$C_{65}H_{59}BCl_2F_4NOOsP_3$ ·2CH_2Cl_2	$C_{62}H_{56}BCl_2F_4N2OOsP_3$ ·CH_2ClCH_2Cl	$C_{67}H_{57}BCl_2F_4NOOsP_3$ ·2.5CH_2Cl_2
M_r	1353.41	1508.86	1480.80	1384.86	1499.23
color	yellow	yellow	yellow-green	green	yellow
T [K]	173(2)	173(2)	173(2)	173(2)	173(2)
radiation ($Mo_{K\alpha}$) [Å]	0.71073	0.71073	0.71073	0.71073	0.71073
crystal system	monoclinic	monoclinic	triclinic	monoclinic	monoclinic
space group	*C2/c*	*P21/c*	*P*-1	*P21/n*	*P21/c*
a [Å]	46.106(9)	20.932(4)	11.461(2)	12.256(3)	13.7362(3)
b [Å]	11.724(2)	11.285(2)	16.474(3)	20.869(4)	26.8114(8)
c [Å]	24.024(5)	28.041(6)	17.603(4)	23.522(5)	17.7918(5)
α [°]	90.00	90.00	92.47(3)	90.00	90.00
β [°]	111.59(3)	99.18(3)	100.28(3)	93.64(3)	98.656(2)
γ [°]	90.00	90.00	101.12(3)	90.00	90.00
V Å^3	12074(4)	6539(2)	3198.5(11)	6004(2)	6477.8(3)
Z	8	4	2	4	4
ρ_{calcd} [g cm^{-3}]	1.489	1.533	1.538	1.532	1.537
μ [mm^{-1}]	2.380	2.324	2.374	2.438	2.386
F(000)	5448	3040	1488	2784	3008
crystal size [mm]	0.25×0.15×0.1	0.2×0.15×0.05	0.2×0.1×0.05	0.5×0.3×0.2	0.5×0.4×0.4
reflns collected	45262	45829	25175	41018	31770
independent reflns	10606	11481	11228	10367	11398
observed reflns ($I \geq 2\sigma(I)$)	7242	9003	8217	8593	8750
data/restraints/parameters	10606/0/731	11481/12/755	11228/12/743	10367/6/721	11398/9/766
GOF on F^2	0.877	1.141	1.150	1.094	1.151
R_1/wR_2 [$I \geq 2\sigma(I)$]	R_1 = 0.0741, wR_2 = 0.1853	R_1 = 0.0520, wR_2 = 0.1295	R_1 = 0.0710, wR_2 = 0.1683	R_1 = 0.0413, wR_2 = 0.0863	R_1 = 0.0637, wR_2 = 0.1452
R_1/wR_2 (all data)	R_1 = 0.1161, wR_2 = 0.2517	R_1 = 0.0721, wR_2 = 0.1571	R_1 = 0.1101, wR_2 = 0.2265	R_1 = 0.0586, wR_2 = 0.1040	R_1 = 0.0886, wR_2 = 0.1548
Largest peak/hole [e Å^{-3}]	2.248 and −3.436	1.984 and −1.912	2.235 and −3.055	0.817 and −1.082	2.001 and −1.288

Table 2. Selected bond lengths [Å] and angles [°] for **2a**, **3a**, **4a**, **4b**, and **5**.

	2a	**3a**	**4a**	**4b**	**5**
Os1–C1	1.962(10)	1.780(7)	2.095(11)	2.074(4)	1.978(7)
Os1–N1	1.918(11)	2.082(6)	1.806(10)	1.812(4)	2.053(6)
C1–C2	1.417(15)	1.365(10)	1.350(16)	1.349(6)	1.356(9)
C2–C3	1.447(16)	1.547(10)	1.533(15)	1.534(6)	1.546(9)
C3–C4	1.460(15)	1.518(10)	1.550(15)	1.504(6)	1.491(9)
C4=N1	1.299(16)	1.272(9)	1.261(15)	1.267(6)	1.278(9)
C1-Os1-N1	85.3(4)	79.0(3)	79.2(5)	78.43(17)	84.2(2)
Os1-C1-C2	128.6(8)	150.5(6)	128.8(9)	130.7(3)	133.1(5)
C1-C2-C3	125.8(10)	115.2(6)	127.2(10)	127.0(4)	123.5(6)
C2-C3-C4	118.1(10)	114.7(6)	109.0(9)	111.5(4)	112.9(6)
C3-C4-N1	121.0(11)	124.3(7)	116.7(10)	119.0(4)	123.5(6)
C4-N1-Os1	139.4(9)	135.1(5)	152.5(8)	152.9(3)	134.8(5)

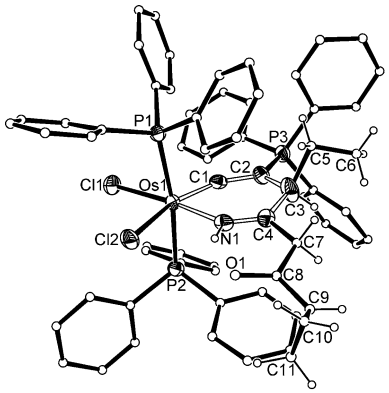

Figure 2. Molecular structure of **3a**. The hydrogen atoms of PPh_3 are omitted for clarity.

even smaller than those of reported six-membered iso-metallabenzenes (155.1(8)°[5b] and 158.5(3)°[5c] and iso-metallabenzenones (152.7(5)° and 151.1(2)°).[6] This is further support that resonance form **3A** is an important contribution to the overall structure of complex **3a**.

To understand the mechanistic aspects of the formation of **2a** and **3a**, we initially performed the same experiment at RT to capture the reaction intermediates. As shown in Scheme 3, when a solution of **1** and excess 3-cyclopropyl-3-oxopropanenitrile in $CHCl_3$ was stirred at RT for 1 h, **1** was completely consumed to afford **4a** as the dominant product. Experimentally, **4a** can be converted to **2a** or **3a**, thus supporting **4a** as the key reaction intermediate. When a solution of **4a** in $CHCl_3$ was stirred at reflux temperature for 12 h, complex **2a** was isolated in 73% yield. When a solution of **4a** in $CHCl_3$ was heated at reflux temperature in the presence of added HCl the conversion was complete within 3 h and **3a** was the major product (Scheme 3).

Complex **4a** was isolated as a green solid in 70% yield. It was characterized by HRMS, multinuclear NMR spectroscopy, and single-crystal X-ray diffraction analysis. A view of the complex cation is shown in Figure 3. The X-ray indicates that **4a**

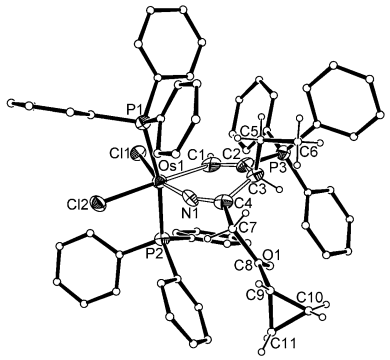

Figure 3. Molecular structure of **4a**. The hydrogen atoms of PPh_3 are omitted for clarity.

contains a metal–azavinylidene moiety (Os=N=C) inside a six-membered osmacycle. The Os1=N1 bond length (1.806(10) Å) is within the typical range of bond lengths for azavinylidene–osmium complexes (1.777–1.881 Å),[8i–k,m–n,16] and the N1=C4 bond length (1.261(15) Å) is in the expected range for C=N double-bond lengths. The Os1–C1 (2.095(11) Å) and C1=C2 (1.350(16) Å) bond lengths are similar to those found in other osmium–vinyl metallacycles[5b,14,17,18] and support the presence of a vinyl moiety. In contrast to the metallacycles in **2a** and **3a**, that in complex **4a** clearly deviates from planarity, which is reflected by the sum of the angles in the six-membered ring (713.4°). The mean deviation from the least-squares plane through the chain of five atoms (C2, C1, Os1, N1, and C4) is 0.0321 Å. The C3 atom is out of the plane of the other metallacyclic atoms by 0.385 Å.

Taking into account all of the above observations, we present a plausible mechanism (Scheme 4). A 1,2-hydrogen-atom shift from the osmium center to the carbyne carbon atom of **1** leads to the formation of alkenylcarbene intermediate **A**. The transformation of the hydrido-alkenylcarbyne to an alkenylcarbene and the influence of the co-ligands on the transformation have been thoroughly studied by Esteruelas et al.[19] Coordination of a nitrile molecule to **A** gives **B**, which can undergo formal [4+2] cyclization to form the six-membered iso-metallapyridinium **4**. Subsequent dissociation of H^+ from the γ-carbon atom affords the aromatic osmapyridine **C**, which can instantly combine with the HBF_4 byproduct to give osmapyridinium **2**. Protonation of the nitrogen atom of **4** and spontaneous proton loss from C1 with (or without) migration to the metal atom in subsequent steps leads to the formation of iso-osmapyridinium **3**. The similar conversion of alkenyl complexes to hydride-vinylidene complexes by α-elimination is a well-known process.[20] Under these reaction conditions, it is likely that excess HCl can promote the formation of **3**. Consistent with the proposed mechanism, the addition of excess HCl could suppress the formation of **2** and thus facilitate the formation of **3** (Scheme 3).

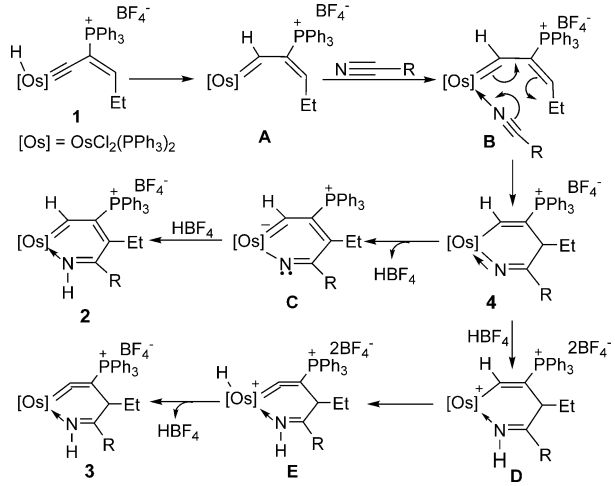

Scheme 4. Proposed mechanism for the formation of **2**–**4**.

Reactions of hydrido-butenylcarbyne complex 1 with 2-cyanoacetamide

We previously demonstrated that hydrido-butenylcarbyne complex **1** can convert to a metallabenzene by three hydrogen eliminations in the presence of air and excess 2-cyanoacetamide at reflux temperature.[12] Heating a mixture of **1** and excess 2-cyanoacetamide in $CHCl_3$ at reflux temperature in the presence of HCl produced a red-brown solution. The ^1H NMR spectrum recorded in situ indicates that the reaction generated a complex mixture of species. However, the reaction in the presence of HI led to the formation of paramagnetic complex **5** (Scheme 5), which could be isolated from the reaction mixture as a yellow solid in 55% yield.

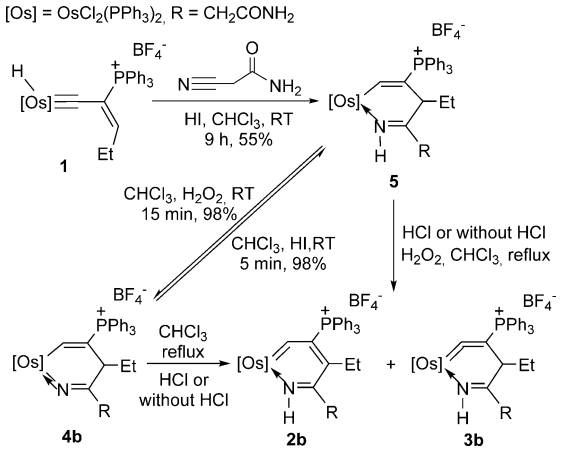

Scheme 5. Reactions of **1** with 2-cyanoacetamide.

Complex **5** was characterized by single-crystal X-ray diffraction analysis, HRMS and elemental analysis. The crystallographic details are given in Table 1 and selected bond lengths and angles are given in Table 2. The X-ray indicates that **5** also contains a six-membered metallacycle (Figure 4). The metallacycle of **5** differs from the metallacycle of **4a** in that the Os–N bond length in **5** (2.053(6) Å) is considerably longer than in **4a** (1.806(10) Å). Nevertheless, we were not able to detect the signal of an analogue of **4a** by in situ ^1H NMR spectroscopy. It

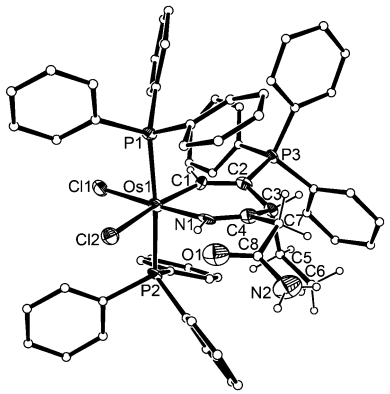

Figure 4. Molecular structure of **5**. The hydrogen atoms of PPh_3 are omitted for clarity.

appears that addition of HI facilitates the formation of paramagnetic complex **5**.

Interestingly, conversion of **5** to the six-membered azavinylidene–osmium complex **4b** was assisted by the oxidant H_2O_2 (Scheme 5). The structure of **4b** was confirmed by X-ray diffraction (Figure 5) Complexes **4b** and **5** have similar overall

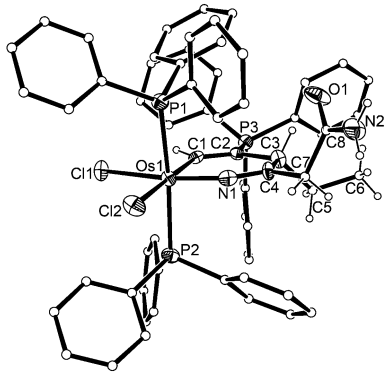

Figure 5. Molecular structure of **4b**. The hydrogen atoms of PPh_3 are omitted for clarity.

structural features, except for the bonding pattern between the metal center and nitrogen atom. Experimentally, **4b** is easily reduced in the presence of HI to generate the reduction product **5** (Scheme 5). We have also carried out the reactions of **4b** with HCl or without HCl at reflux temperature in $CHCl_3$. As shown in Scheme 5, the conversion of **4b** to **2b** and **3b** was observed. Complexes **2b** and **3b** can also be formed by addition of H_2O_2 to **5**. Complexes **2b**, **3b**, and **4b** were characterized by NMR spectroscopy (in part), elemental analysis, and HRMS. The attempt to obtain full NMR spectroscopic characterization of these complexes failed due to their poor solubility in ordinary organic solvents. The similarity of their observable NMR spectroscopic data suggests that complexes **2b**, **3b**, and **4b** have structures similar to those of **2a**, **3a**, and **4a**.

Reactions of hydrido-butenylcarbyne complex 1 with 2-formylbenzonitrile

After the successful preparation of osmapyridinium **2b** and iso-osmapyridinium **3b** from the reaction of hydrido-butenylcarbyne complex **1** with 2-cyanoacetamide, we next examined the reaction of **1** with 2-formylbenzonitrile. Treatment of **1** with excess 2-formylbenzonitrile in $CHCl_3$, followed by addition of HI, produced paramagnetic complex **6** with isolated yields of 30% (Scheme 6). Paramagnetic complex **6** is also reac-

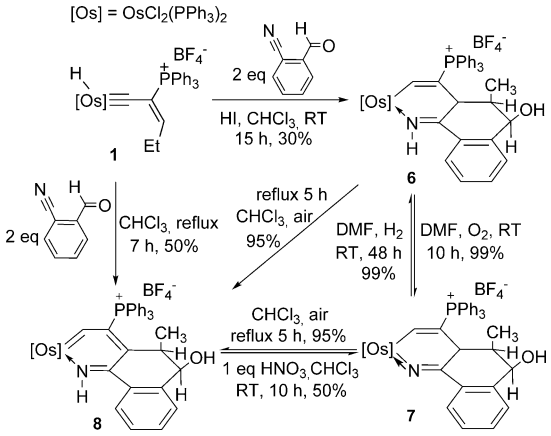

Scheme 6. Reactions of **1** with 2-formylbenzonitrile.

tive to oxidant treatment. Due to its poor solubility in common organic solvents, we stirred a solution of **6** in DMF under an O_2 atmosphere and found that **6** can be almost completely converted to **7** at RT within 10 h (Scheme 6). Complex **7** was identified as the expected product derived from the oxidation reaction of **6**. Additionally, the conversion of **7** to **6** proceeds smoothly by stirring a solution of **7** in DMF under an H_2 atmosphere for 48 h.

The structures of **6** and **7** have been confirmed by X-ray diffraction. The crystallographic details are given in Table 3 and selected bond lengths and angles are given in Table 4. As shown in Figures 6 and 7, both complexes contain a tricyclic skeleton composed of three fused six-membered rings. The two Os–N bond lengths in each of the complexes are clearly different: the Os=N bond in **7** (1.808(8) Å) is shorter than that the Os–N bond in **6** (2.000(7) Å). The X-ray study also confirms the *cis* orientation of the methyl and hydroxyl groups in the rings. The metallacycles in **6** and **7** are similar to those in paramagnetic complex **5** and iso-osmapyridinium **4**. It appears that the ethyl substituents of the starting carbyne complex **1** react with the formyl group of 2-formylbenzonitrile to form the final fused six-membered ring of **6**, although the exact mechanism is still not clear to us. It is possible that the stability of the final product is important to induce formation of the fused metallacycle.

As expected, when **6** was stirred in DMF under a nitrogen atmosphere no appreciable formation of **7** was observed. However, heating **6** at reflux temperature in $CHCl_3$ in the presence

Table 3. Crystal data and structure refinement for **6**–**11**.

	6·$2CH_2Cl_2$	**7**·$2CH_2Cl_2$	**8**·$2CH_2Cl_2$	**9**·C_6H_6	**10**·$3CH_2Cl_2$	**11**·$0.5CH_2ClCH_2Cl$·$4H_2O$
formula	$C_{67}H_{58}BCl_2F_4NOOsP_3$·$2CH_2Cl_2$	$C_{67}H_{57}BCl_2F_4NOOsP_3$·$2CH_2Cl_2$	$C_{67}H_{57}BCl_2F_4NOOsP_3$·$2CH_2Cl_2$	$C_{67}H_{53}BCl_2F_4NOOsP_3$·$C_6H_6$	$C_{49}H_{38}Cl_3NOOsP_2$·$3CH_2Cl_2$	$C_{49}H_{38}Cl_2INOOsP_2$ $0.5CH_2ClCH_2Cl$·$4H_2O$
M_r	1503.82	1502.81	1502.81	1407.03	1270.07	1228.28
color	yellow	yellow-green	yellow	yellow	purple	purple
T [K]	173(2)	173(2)	173(2)	143(2)	173(2)	173(2)
radiation ($Mo_{K\alpha}$) [Å]	0.71073	0.71073	0.71073	0.71073	0.71073	0.71073
crystal system	monoclinic	monoclinic	monoclinic	monoclinic	monoclinic	monoclinic
space group	*P*21/*n*	*P*21/*n*	*P*21/*n*	*P*21/*n*	*P*21/*c*	*P*21/*c*
a [Å]	16.418(3)	16.133(3)	16.1571(5)	16.0143(5)	16.797(3)	16.997(3)
b [Å]	20.562(4)	20.592(4)	20.5748(6)	20.1135(8)	12.911(3)	13.101(3)
c [Å]	18.999(4)	19.352(4)	18.9779(6)	19.1984(8)	24.930(5	25.517(5)
α [°]	90.00	90.00	90.00	90.00	90.00	90.00
β [°]	91.77(3)	94.64(3)	91.985(2)	94.590(3)	106.81(3)	107.66(3)
γ [°]	90.00	90.00	90.00	90.00	90.00	90.00
V [Å^3]	6411(2)	6408(2)	6305.0(3)	6164.0(4)	5175.5(18)	5414.4(19)
Z	4	4	4	4	4	4
ρ_{calcd} [g cm^{-3}]	1.558	1.558	1.583	1.516	1.630	1.485
μ, [mm^{-1}]	2.371	2.372	2.410	2.292	3.030	3.172
F(000)	3020	3016	3016	2832	2520	2380
crystal size [mm]	0.2×0.15×0.05	0.1×0.1×0.05	0.5×0.4×0.3	0.25×0.15×0.1	0.2×0.15×0.1	0.2×0.1×0.05
reflns collected	47 676	59 829	30 267	31 672	37 384	30 383
independent reflns	11 262	11 027	11 088	10 829	9087	9388
observed reflns ($I \geq 2\sigma(I)$)	7754	7869	6763	7733	5689	6936
data/restraints/parameters	11 262/6/821	11 027/48/775	11 088/182/811	10 829/48/763	9087/0/584	9388/60/584
GOF on F^2	1.157	0.990	0. 865	1.046	1.044	1.069
R_1/wR_2 [$I \geq 2\sigma(I)$]	R_1 = 0.0547, wR_2 = 0.1279	R_1 = 0.0696, wR_2 = 0.1879	R_1 = 0.0469, wR_2 = 0.0911	R_1 = 0.0670, wR_2 = 0.1447	R_1 = 0.0652, wR_2 = 0.1513	R_1 = 0.0659, wR_2 = 0.2051
R_1/wR_2 (all data)	R_1 = 0.0926, wR_2 = 0.1786	R_1 = 0.1019, wR_2 = 0.2043	R_1 = 0.0874, wR_2 = 0.0981	R_1 = 0.1044, wR_2 = 0.1620	R_1 = 0.1093, wR_2 = 0.1777	R_1 = 0.0931, wR_2 = 0.2255
Largest peak/hole [e Å^{-3}]	1.366 and −1.589	2.777 and −1.612	2.070 and −1.846	2.264 and −1.349	1.470 and −1.877	2.675 and −1.589

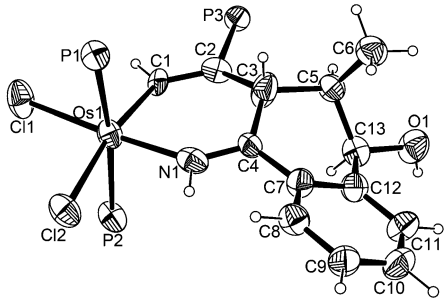

Figure 6. Molecular structure of **6**. The phenyl groups of PPh_3 and some of the hydrogen atoms are omitted for clarity.

of air led to the formation of complex **8** after efficient aromatization of the six-membered metallacycle. Complex **8** was also obtained as the major product after heating hydrido-butenylcarbyne complex **1** and excess 2-formylbenzonitrile in $CHCl_3$. Complex **8** has been fully characterized by NMR spectroscopy, elemental analysis, HRMS, and single-crystal X-ray diffraction. The molecular structure of complex **8** is shown in Figure 8. Complex **8** contains an essentially planar six-membered osmapyridinium ring. The mean deviation from the least-squares plane through Os1, C1–C4, and N1 is 0.0155 Å. The maximum deviation from the least-squares plane through Os1, C1–C4, and N1 is 0.0280 Å for C3. As shown in Table 3, the C–C bond

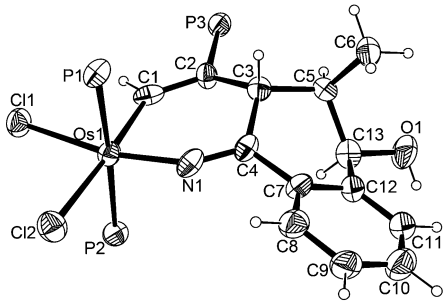

Figure 7. Molecular structure of **7**. The phenyl groups of PPh_3 and some of the hydrogen atoms are omitted for clarity.

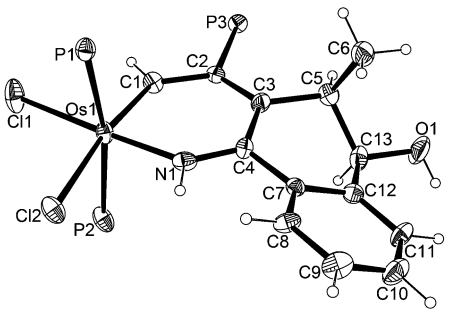

Figure 8. Molecular structure of **8**. The phenyl groups of PPh_3 and some of the hydrogen atoms are omitted for clarity.

Table 4. Selected bond lengths [Å] and angles [°] for **6**–**11**.

	6	7	8	9	10	11
Os1–C1	1.984(8)	2.072(10)	1.922(6)	2.078(9)	1.777(9)	1.765(10)
Os1–N1	2.000(7)	1.808(8)	1.946(5)	1.747(8)	1.994(8)	2.025(7)
C1–C2	1.357(10)	1.383(13)	1.408(8)	1.350(13)	1.380(11)	1.394(13)
C2–C3	1.523(12)	1.527(13)	1.410(9)	1.527(12)	1.503(11)	1.466(12)
C3–C4	1.484(12)	1.549(13)	1.441(9)	1.505(12)	1.471(11)	1.504(13)
C4=N1	1.304(9)	1.256(12)	1.310(8)	1.268(11)	1.297(10)	1.308(12)
C3–C5	1.566(10)	1.566(13)	1.522(9)	1.372(13)	1.340(11)	1.369(13)
C5–C13	1.528(12)	1.556(14)	1.554(9)	1.474(12)	1.500(12)	1.459(15)
C13–C12	1.504(12)	1.502(14)	1.513(9)	1.459(14)	1.466(14)	1.474(16)
C12=C7	1.398(11)	1.400(14)	1.406(9)	1.346(13)	1.395(12)	1.371(14)
C7–C4	1.462(11)	1.485(13)	1.478(9)	1.485(11)	1.469(11)	1.453(13)
C12–C11	1.390(12)	1.372(14)	1.389(9)	1.420(12)	1.393(11)	1.398(15)
C11–C10	1.386(13)	1.399(16)	1.365(10)	1.345(15)	1.377(14)	1.410(19)
C10–C9	1.373(12)	1.388(17)	1.383(10)	1.393(15)	1.384(16)	1.390(18)
C9–C8	1.379(12)	1.379(14)	1.364(9)	1.341(12)	1.382(14)	1.370(16)
C8–C7	1.398(12)	1.416(14)	1.394(9)	1.400(13)	1.386(13)	1.388(15)
C1-Os1-N1	84.4(3)	80.4(4)	87.0(2)	77.7(3)	78.4(3)	79.1(3)
Os1-C1-C2	132.3(6)	129.0(7)	129.8(5)	130.3(7)	148.1(6)	148.5(7)
C1-C2-C3	123.5(7)	126.0(8)	125.1(6)	125.4(8)	115.5(7)	115.3(7)
C2-C3-C4	116.9(7)	110.1(7)	120.5(6)	111.9(8)	115.1(7)	117.4(8)
C3-C4-N1	120.0(7)	118.2(8)	122.0(6)	116.9(7)	121.7(7)	120.3(8)
C4-N1-Os1	138.2(6)	150.9(7)	135.5(5)	155.7(6)	138.3(6)	137.1(6)
C4-C3-C5	112.2(7)	110.3(8)	114.9(6)	116.4(8)	119.1(8)	116.5(8)
C3-C5-C13	110.3(7)	111.3(8)	108.8(5)	120.7(9)	121.0(9)	122.0(9)
C5-C13-C12	110.1(6)	110.5(8)	108.6(5)	121.1(9)	118.5(9)	119.1(9)
C13-C12-C7	117.5(7)	115.9(9)	118.3(6)	120.3(9)	120.5(8)	120.3(9)
C12-C7-C4	117.2(8)	118.0(9)	119.0(6)	118.9(9)	118.1(8)	118.8(9)
C7-C4-C3	120.9(7)	120.4(8)	120.0(6)	121.4(8)	120.9(7)	120.9(8)
C7-C12-C11	119.2(7)	119.4(10)	119.8(7)	120.0(9)	120.6(10)	120.8(11)
C12-C11-C10	120.2(8)	119.6(10)	120.0(7)	118.9(10)	119.7(9)	120.2(11)
C11-C10-C9	121.0(8)	121.6(10)	120.8(7)	120.4(9)	119.7(9)	117.8(11)
C10-C9-C8	119.5(9)	119.5(11)	119.7(7)	121.0(10)	120.9(11)	121.1(12)
C9-C8-C7	120.7(9)	119.0(10)	121.2(7)	119.3(10)	120.0(10)	121.3(11)
C8-C7-C12	119.5(8)	120.9(9)	118.3(6)	120.4(8)	119.0(8)	118.8(9)

lengths in the osmapyridinium ring also support a predominantly delocalized electronic arrangement. The bond length of the bridging carbon atoms (C3–C4 1.441(9) Å) is slightly longer than other C–C bonds in the metallacycle.

Structurally, the dehydration reaction of osmapyridinium **8** should afford a benzo-osmaquinoline complex. However, **8** is unreactive to treatment with acids such as H_2SO_4, HBF_4, and HCl at RT. The reaction of **8** with other dehydration agents also failed to achieve the desired dehydration product. For example, the reaction with acetic anhydride only led to the alcoholysis product. Interestingly, osmapyridinium **8** was converted into iso-osmapyridinium **7** after stirring with HNO_3 (1 equiv) at RT for several hours (Scheme 6). When treated with HNO_3 (4 equiv), the hydroxyl group of **8** was oxidized to produce iso-osmapyridinium **9** with a fused naphthalenone fragment (Scheme 7); the structure of **9** was confirmed by X-ray analysis.

As shown in Figure 9, a bonding pattern similar to that depicted for **V** (Scheme 1) was found for the iso-osmapyridinium ring of complex **9**. Similar to iso-osmapyridiniums **4** and **7**, the metallacycle of **9** also shows little deviation from planarity, which is reflected by the mean deviation from the least-squares plane through the six atoms of the metallacycle (0.0672 Å). The dihedral angle of the metallacycle with respect to the fused naphthalenone fragment in complex **9** is 14.6°, most likely due to the repulsive interaction between the methyl and phosphonium substituents. The ring C–C bond lengths are in the range of 1.341–1.527 Å with a clear alternation between double and single bonds, which suggests poor electron delocalization within the tricyclic rings of **9**.

According to the reaction conditions described above, addition of HCl could promote conversion of iso-osmapyridinium **4** to iso-osmapyridinium **3**. We also reacted **9** with hydrogen halides, such as HCl and HI, under similar conditions. As shown in Scheme 7, conversion of iso-osmapyridinium **9** to iso-osmapyridinium **10** proceeded in the presence of HCl at RT, and **10** was isolated as a purple solid in 70% yield. We isolated the analogous iso-osmapyridinium **11** in 40% yield from the reaction of **9** with HI (Scheme 7).

The two complexes were characterized by X-ray diffraction analysis (Figures 10 and 11). Both complexes contain a six-membered iso-osmapyridinium ring fused with a naphthalenone segment. The data in Table 4 shows that the structural parameters associated with the metallacycles of complexes **10** and **11** are similar to those of iso-osmapyridinium **3a**. The Os=C bond lengths in each of the complexes are only very slightly different. Notably, the Os=C bond in **11** (1.765(10) Å) is shorter than for most reported osmium–vinylidene complexes (1.762–1.946 Å).[15] The Os1-C1-C2 angles in **10** and **11** deviate from linearity (148.1(6)° in **10** and 148.5(7)° in **11**) by a smaller amount than in iso-osmapyridinium **3a**. The dihedral angles between the planes of the metallacycles and naphthalenone segments are 17.5° and 17.7° for complexes **10** and **11**, respectively. The considerable distortion of the tricyclic rings in **10** and **11** may be attributed to the li-

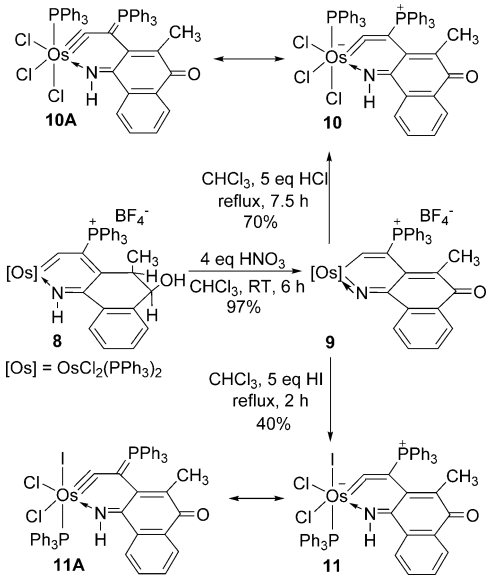

Scheme 7. Conversions of osmapyridinium **8** to the iso-osmapyridiniums **9**–**11**.

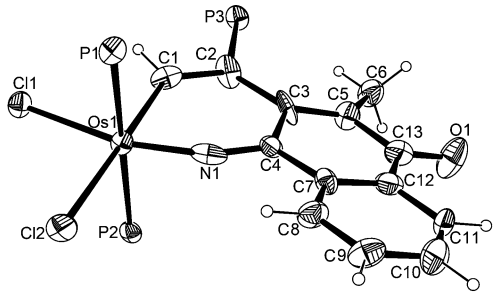

Figure 9. Molecular structure of **9**. The phenyl groups of the PPh_3 groups and some of the hydrogen atoms are omitted for clarity.

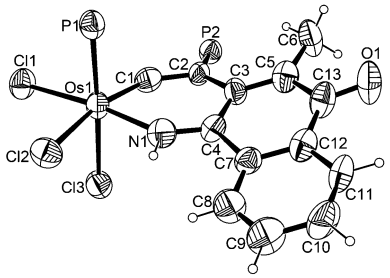

Figure 10. Molecular structure of **10**. The phenyl groups of the PPh_3 groups and some of the hydrogen atoms are omitted for clarity.

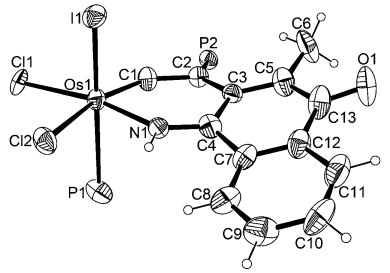

Figure 11. Molecular structure of **11**. The phenyl groups of PPh_3 and some of the hydrogen atoms are omitted for clarity.

gands attached to the metal center. We think that the unsymmetrical ligand environments above and below the metallacycles may create an unsymmetrical steric effect and increase the distortion of the tricyclic rings in **10** and **11**.

DFT studies of aromaticity and strain in the metallacycles

We carried out DFT calculations to evaluate the aromaticity of the metallapyridinium ring of complex **2**. The optimized structure of the model complex **2′**, in which the PPh_3 groups were replaced with PH_3 and the R groups were replaced with CH_3, effectively reproduces the structural features of **2** described above. The nucleus-independent chemical shift (NICS) values were computed for the metallapyridinium ring. The calculated NICS values are $\delta = -7.7$ (NICS(0)) and -11.5 ppm (NICS(1)). These values are comparable to those reported for other metalla-aromatic complexes.[14] The aromatic stabilization energy (ASE) was also evaluated by employing the isomerization method introduced by Schleyer and Pühlhofer.[21] An ASE of 33.7 kcal mol^{-1} was obtained for model complex **2′** (Scheme 8 a). The calculated ASE is higher than for other metalla-aromatic complexes.[14] The negative NICS values and the calculated ASE indicate that the metallapyridium ring in complex **2** is aromatic.

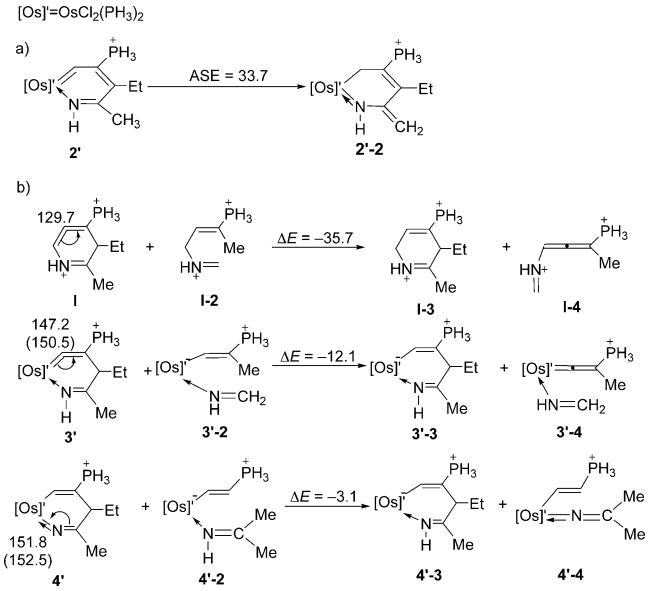

Scheme 8. a) The calculated aromatic stabilization energies [kcal mol^{-1}] for complex **2′**; b) the calculated strain energies [kcal mol^{-1}] of the cations of iso-metallapyridiniums **3′** and **4′** on the basis of the isodesmic reactions. The selected calculated and experimental (in parentheses) bond angles [°] are marked for **I**, **3′**, and **4′**.

Model DFT calculations were also used to estimate the strain differences between the isomers that contained organometallic cumulene, iso-metallapyridinium derivatives **3** and **4**, on the basis of an isodesmic reaction.[22] The optimized structures of model complexes **3′** and **4′**, in which the PPh_3 groups were replaced with PH_3 and the R groups were replaced with CH_3, effectively reproduce the structural features of **3** and **4** described above. The angle of the cumulative double bonds in the parent six-membered iso-pyridinium $[CH{=}C{=}C(PH_3)C(Et)C(Me){-}NH]^{2+}$ was calculated to be 129.7°. This value is much smaller than the angle in model complex **3′** (147.2°). The strain energy of the parent six-membered iso-pyridinium was estimated to be 35.7 kcal mol^{-1}. In sharp contrast, the computationally derived strain energy of model complex **3′** is significantly smaller (12.1 kcal mol^{-1}). Furthermore, in the case of model complex **4′**, the strain energy was calculated to be 3.1 kcal mol^{-1}.[23] These DFT results agree well with previous reports, which showed that introduction of a transition-metal atom or a main-group heteroatom is an efficient strategy to reduce the inherent ring strain in cycloallenes.[6,24]

Conclusion

The reaction of hydrido-butenylcarbyne complex **1** with nitriles revealed the formation of six-membered osmacycles that con-

tained vinylidene and azavinylidene moieties. These metallacycles may be also described as the first examples of iso-metallapyridinium complexes. The formal [4+2] synthetic strategy described can be extended to produce iso-metallapyridiniums with a fused naphthalenone fragment by the reaction of hydrido-butenylcarbyne complex **1** with 2-formylbenzonitrile. Further theoretical studies of the iso-metallapyridinium derivatives suggest that the incorporation of transition-metal moieties can effectively reduce ring strain in the six-membered rings that contain cumulative double bonds.

Experimental Section

General comments

All manipulations were performed at RT under a nitrogen atmosphere by using standard Schlenk techniques unless otherwise stated. Solvents were distilled from sodium/benzophenone (hexane and diethyl ether) or calcium hydride (dichloromethane and $CHCl_3$) under a nitrogen atmosphere prior to use. Other reagents were used as received from commercial sources without further purification. NMR spectroscopic experiments were performed with a Bruker AVIII- 500 (^{1}H: 500.2 MHz; ^{13}C: 125.8 MHz; ^{31}P: 202.5 MHz) or Bruker AV-400 spectrometer (^{1}H: 400.1 MHz; ^{13}C: 100.2 MHz; ^{31}P: 162.0 MHz). ^{1}H and ^{13}C NMR chemical shifts are reported relative to TMS, and ^{31}P NMR chemical shifts are reported relative to 85% H_3PO_4 in H_2O. When required HSQC, HMQC, and DEPT-135 experiments were used to assist the characterization. Elemental analyses were performed with a Vario EL III elemental analyzer. HRMS experiments were performed with a Bruker En Apex Ultra 7.0T FT-M instrument.

Complex 2a

Method a: In a Schlenk tube, a solution of **1** (200 mg, 0.166 mmol) and 3-cyclopropyl-3-oxopropanenitrile (32 μL, 0.33 mmol) in $CHCl_3$ (10 mL) was heated at reflux temperature for approximately 12 h to produce a yellow solution. The solution was concentrated under vacuum to a volume of approximately 1 mL. Addition of diethyl ether (20 mL) to the solution afforded a yellow precipitate, which was collected by filtration, washed with diethyl ether (2×15 mL), and then washed with dichloromethane (2 mL) and diethyl ether (20 mL) three times. The yellow solid was dried under vacuum to give **2a** (155 mg, 71%).

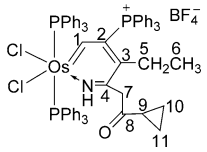

Method b: In a Schlenk tube, a solution of **4a** (197 mg, 0.150 mmol) in $CHCl_3$ (10 mL) was heated at reflux temperature for 12 h to produce a yellow solution. The solution was concentrated under vacuum to a volume of approximately 1 mL. Addition of diethyl ether (20 mL) to the solution afforded a yellow precipitate, which was collected by filtration, washed with diethyl ether (2× 15 mL), and then washed with dichloromethane (2 mL) and diethyl ether (20 mL) three times. The yellow solid was dried under vacuum to give **2a** (144 mg, 73%). ^{1}H NMR (500.2 MHz, CD_2Cl_2): δ = 39.0 (d, J(P,H) = 19.4 Hz, 1H; C^1*H*), 24.4 (s, 1H; N*H*), 7.7–6.9 (m, 45H; Ph), 2.9 (br, 2H; C^7*H*), 1.7 (br, 1H; C^9*H*), 1.2 (br, 2H; C^5*H*), 0.9 (br, 2H; C^{10}*H*), 0.8 (br, 2H; C^{11}*H*), 0.2 ppm (m, J(H,H) = 6.9 Hz, 3H; C^6*H*); ^{13}C NMR: poor solubility of **2a** prevented characterization by ^{13}C NMR spectroscopy; ^{31}P NMR (202.5 MHz, CD_2Cl_2): δ = 17.2 (s; C(*P*Ph$_3$)), 1.1 ppm (s; Os*P*Ph$_3$); HRMS (ESI): *m/z* calcd for $[C_{65}H_{59}Cl_2NOOsP_3]^+$: 1224.2796 $[M]^+$, found: 1224.2788; elemental analysis calcd (%) for $C_{65}H_{59}Cl_2NOP_3BF_4Os$: C 59.55, H 4.54, N 1.07; found: C 59.46, H 4.41, N 1.10.

Complex 3a

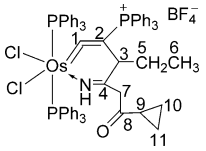

Method a: HCl (66 μL, 0.80 mmol) and 3-cyclopropyl-3-oxopropanenitrile (30 μL, 0.31 mmol) were added to a solution of **1** (192 mg, 0.160 mmol) in $CHCl_3$ (10 mL). The mixture was heated at reflux temperature for 4 h under a nitrogen atmosphere. The reaction mixture was concentrated under vacuum to a volume of approximately 1 mL. Addition of diethyl ether (20 mL) to the residue afforded a yellow precipitate, which was collected by filtration, washed with diethyl ether (2×15 mL), and then washed with methanol (2×2 mL) The yellow solid was dried under vacuum to give **3a** (132 mg, 63%).

Method b: HCl (62 μL, 0.75 mmol) was added to a solution of **4a** (197 mg, 0.150 mmol) in $CHCl_3$ (10 mL). The mixture was heated at reflux temperature for 3 h under a nitrogen atmosphere. The reaction mixture was then concentrated under vacuum to a volume of approximately 1 mL. Addition of diethyl ether (20 mL) to the residue afforded a yellow precipitate, which was collected by filtration, washed with diethyl ether (2×15 mL), and then washed with methanol (2×2 mL). The yellow solid was dried under vacuum to give **3a** (128 mg, 65%). ^{1}H NMR (500.2 MHz, CD_2Cl_2): δ = 12.4 (s, 1H; N*H*), 7.7–6.9 (m, 45H; Ph), 3.8 (br, 1H; C^3*H*), 3.1 (d, J(H,H) = 22.0 Hz, 1H; C^7*H*), 2.8 (d, J(H,H) = 22.0 Hz, 1H; C^7*H*), 1.8 (m, 1H; C^9*H*), 1.0 (m, 2H; C^{10}*H*), 0.9 (m, 2H; C^{11}*H*), 0.8 (m, 1H; C^5*H*), 0.3 (m, 1H; C^5*H*), −0.1 ppm (t, J(H,H) = 7.4 Hz, 3H; C^6*H*); ^{13}C NMR (125.8 MHz, CD_2Cl_2): δ = 271.3 (br; C^1), 208.0 (s; C^8), 173.0 (d, J(P,C) = 5.1 Hz; C^4), 135.5–128.5 (m, Ph), 122.3 (d, J(P,C) = 83.6 Hz; C^2), 45.9 (s; C^7), 41.3 (d; J(P,C) = 11.2 Hz; C^3), 30.8 (s; C^5), 22.1 (s; C^9), 13.1 (s; C^{10}), 13.0 (s; C^{11}), 12.9 ppm (s; C^6); ^{31}P NMR (202.5 MHz, CD_2Cl_2): δ = 3.6 (s; C(*P*Ph$_3$)), −12.4 (s; Os*P*Ph$_3$), −12.5 ppm (s; Os*P*Ph$_3$); HRMS (ESI): *m/z* calcd for $[C_{65}H_{59}Cl_2NOOsP_3]^+$: 1224.2796 $[M]^+$; found: 1224.2791; elemental analysis calcd (%) for $C_{65}H_{59}Cl_2NOP_3BF_4Os$: C 59.55, H 4.54, N 1.07; found: C 59.51, H 4.43, N 1.15.

Complex 4a

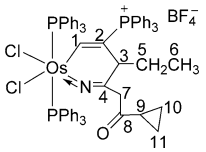

A mixture of **1** (481 mg, 0.400 mmol) and 3-cyclopropyl-3-oxopropanenitrile (78 μL, 0.80 mmol) in $CHCl_3$ (20 mL) was stirred at RT for 1 h under a nitrogen atmosphere. The reaction mixture was concentrated under vacuum to a volume of approximately 2 mL. Addition of diethyl ether (20 mL) to the residue afforded a yellow precipitate, which was collected by filtration, washed with methanol (2 mL) and diethyl ether (25 mL) three times. The green solid was dried under vacuum to give **4a** (367 mg, 70%). ^{1}H NMR (500.2 MHz, CD_2Cl_2): δ = 12.0 (d, J(P,H) = 31.5 Hz, 1H; C^1*H*), 7.8–6.9 (m, 45H; Ph), 6.5 (br, 1H; C^3*H*), 5.2 (d, J(H,H) = 18.9 Hz, 1H; C^7*H*), 3.8 (d, J(H,H) = 18.9 Hz, 1H; C^7*H*), 1.7 (m, 1H; C^9*H*), 1.0 (m, 1H; C^5*H*), 0.9 (m, 2H; C^{10}*H*), 0.7 (m, 2H; C^{11}*H*), 0.6 (m, 1H; C^5*H*), 0.1 ppm (t, J(H,H) = 7.1 Hz, 3H; C^6*H*); ^{31}P NMR (202.5 MHz, CD_2Cl_2): δ = 17.1 (s; C(*P*Ph$_3$)), −25.0 (d, J(P,P) = 387.8 Hz; Os*P*Ph$_3$), −28.7 ppm (d, J(P,P) = 387.8 Hz; Os*P*Ph$_3$); ^{13}C NMR (125.8 MHz, CD_2Cl_2): δ = 207.4 (s; C^8),

180.9 (br; C^1), 140.0 (d, J(P,C) = 11.0 Hz; C^4), 134.8–119.8 (m; Ph), 109.5 (d, J(P,C) = 71.5 Hz; C^2), 35.4 (d, J(P,C) = 23.6 Hz; C^3), 34.2 (s; C^5), 30.2 (s; C^7), 20.1 (s; C^9), 12.8 (s; C^6), 12.5 (s; C^{10}), 11.8 (s; C^{11}); HRMS (ESI): *m/z* calcd for $[C_{65}H_{59}Cl_2NOOsP_3]^+$: 1224.2796 $[M]^+$; found: 1224.2785; elemental analysis calcd (%) for $C_{65}H_{59}Cl_2NOP_3BF_4Os$: C 59.55, H 4.54, N 1.07; found: C 59.48, H 4.68, N 1.19.

Complex 2b

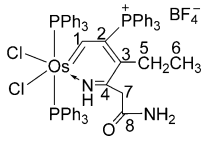

Method a: In a Schlenk tube, a solution of H_2O_2 (76 μL, 0.75 mmol) was added to a solution of **5** (197 mg, 0.154 mmol) in $CHCl_3$ (10 mL). The reaction mixture was heated at reflux temperature for approximately 7 h to produce a yellow solution. The solution was concentrated under vacuum to a volume of approximately 1 mL. Addition of diethyl ether (20 mL) to the solution afforded a yellow precipitate, which was collected by filtration, washed with diethyl ether (2×15 mL), and then washed with dichloromethane (5 mL) and diethyl ether (15 mL) three times. The yellow solid was dried under vacuum to give **2b** (79 mg, 40%).

Method b: In a Schlenk tube, a solution of compound **4b** (201 mg, 0.156 mmol) in $CHCl_3$ (10 mL) was heated at reflux temperature for 6 h to produce a yellow solution. The solution was concentrated under vacuum to a volume of approximately 1 mL. Addition of diethyl ether (20 mL) to the solution afforded a yellow precipitate, which was collected by filtration, washed with diethyl ether (2× 15 mL), and then washed with dichloromethane (5 mL) and diethyl ether (15 mL) three times. The yellow solid was dried under vacuum to give **2b** (110 mg, 55%). ^{1}H NMR (500.2 MHz, CD_2Cl_2): δ = 37.2 (d, J(P,H) = 19.0 Hz, 1H; C^1H), 24.0 (s, 1H; N*H*), 7.7–7.0 (m, 45H; Ph); 6.1 (s, 1H; NH_2), 5.9 (br, 2H; C^7H), 5.6 (s, 1H; NH_2), 1.2 (br, 2H; C^5H), 0.02 ppm (t, J(H,H) = 7.6 Hz, 3H; C^6H); ^{13}C NMR: poor solubility of **2b** prevented characterization by ^{13}C NMR spectroscopy; ^{31}P NMR (202.5 MHz, CD_2Cl_2): δ = 18.4 (s; C(*P*Ph$_3$)), −0.5 (d, J(P,P) = 354.1 Hz; Os*P*Ph$_3$), −15.9 ppm (d, J(P,P) = 354.1 Hz; Os*P*Ph$_3$); HRMS (ESI): *m/z* calcd for $[C_{62}H_{56}Cl_2N_2OOsP_3]^+$: 1199.2592 $[M]^+$; found: 1199.2587; elemental analysis calcd (%) for $C_{62}H_{56}Cl_2N_2P_3BF_4OOs$: C 57.91, H 4.39, N 2.18; found: C 57.86, H 4.02, N 2.12.

Complex 3b

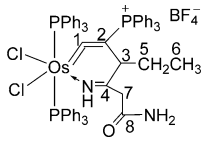

Method a: HCl (68 μL, 0.83 mmol) and H_2O_2 (84 μL, 0.82 mmol) were added to a solution of **5** (228 mg, 0.177 mmol) in $CHCl_3$ (10 mL). The mixture was heated at reflux for 2 h under a nitrogen atmosphere. The reaction mixture was concentrated under vacuum to a volume of approximately 1 mL. Addition of diethyl ether (20 mL) to the residue afforded a yellow precipitate, which was collected by filtration, washed with diethyl ether (2×5 mL), and then washed with acetone (2×2 mL). The yellow solid was dried under vacuum to give **3b** (139 mg, 61%).

Method b: HCl (66 μL, 0.80 mmol) was added to a solution of **4b** (210 mg, 0.163 mmol) in $CHCl_3$ (10 mL). The mixture was heated at reflux temperature for 5 h under a nitrogen atmosphere. The reaction mixture was concentrated under vacuum to a volume of approximately 1 mL. Addition of diethyl ether (20 mL) to the residue afforded a yellow precipitate, which was collected by filtration, washed with diethyl ether (2×5 mL), and then washed with acetone (2×2 mL). The yellow solid was dried under vacuum to give **3b** (143 mg, 68%). ^{1}H NMR (500.2 MHz, CD_2Cl_2): δ = 12.9 (s, 1H; N*H*), 9.0 (s, 1H; NH_2), 7.8–7.0 (m, 45H; Ph), 5.3 (s, 1H; NH_2), 3.9 (br, 1H; C^3H), 3.3 (d, J(H,H) = 19.7 Hz, 1H; C^7H), 2.5 (d, J(H,H) = 19.7 Hz, 1H; C^7H), 1.1 (m, 1H; C^5H), 0.5 (m, 1H; C^5H), 0.05 ppm (t, J(H,H) = 7.6 Hz, 3H; C^6H); ^{13}C NMR: poor solubility of **3b** prevented characterization by ^{13}C NMR spectroscopy; ^{31}P NMR (202.5 MHz, CD_2Cl_2): δ = 3.5 (s; C(*P*Ph$_3$)), −12.1 (s; Os*P*Ph$_3$), −12.6 ppm (s; Os*P*Ph$_3$); HRMS (ESI): *m/z* calcd for $[C_{62}H_{56}Cl_2N_2OOsP_3]^+$: 1199.2592 $[M]^+$; found: 1199.2569; elemental analysis calcd (%) for $C_{62}H_{56}Cl_2N_2P_3BF_4OOs$: C 57.91; H 4.39; N 2.18; found: C 57.96, H 4.02, N 2.39.

Complex 4b

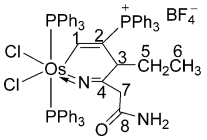

A solution of H_2O_2 (195 μL, 1.9 mmol) was added to a suspension of **5** (502 mg, 0.390 mmol) in $CHCl_3$ (20 mL). The reaction mixture was stirred at RT for 30 min to give a green solution, which was concentrated under vacuum to a volume of approximately 1 mL. Addition of diethyl ether (20 mL) to the residue produced a green precipitate, which was collected by filtration, washed with diethyl ether (2×5 mL), and dried under vacuum to give (492 mg, 98%). ^{1}H NMR (500.2 MHz, CD_2Cl_2): δ = 11.9 (d, J(P,H) = 39.3 Hz, 1H; C^1H), 7.7–6.9 (m, 45H; PPh$_3$), 6.4 (br, 1H; C^3H), 6.1 (s, 1H; NH_2), 5.1 (d, J(H,H) = 21.6 Hz, 1H; C^7H), 5.0 (s, 1H; NH_2), 3.7 (d, J(H,H) = 21.6 Hz, 1H; C^7H), 0.9 (m, 1H; C^5H), 0.4 (m, 1H; C^5H), 0.04 ppm (t, J(H,H) = 8.8 Hz, 3H; C^6H); ^{13}C NMR: poor solubility of **4b** prevented characterization by ^{13}C NMR spectroscopy; ^{31}P NMR (202.5 MHz, CD_2Cl_2): δ = 16.6 (s; C*P*Ph$_3$), −24.4 (d, J(P,P) = 484.0 Hz; Os*P*Ph$_3$), −29.4 ppm (d, J(P,P) = 484.0 Hz; Os*P*Ph$_3$); HRMS (ESI): *m/z* calcd for $[C_{62}H_{56}Cl_2N_2OOsP_3]^+$: 199.2592 $[M]^+$; found: 1199.2599; elemental analysis calcd (%) for $C_{62}H_{56}Cl_2N_2P_3BF_4OOs$: C 57.91, H 4.39, N 2.18; found: C 57.77, H 4.37, N 1.89.

Complex 5

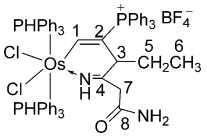

Method a: A solution of HI (128 μL, 0.80 mmol) was added to a solution of **1** (481 mg, 0.40 mmol) and 2-cyanoacetamide (81.7 mg, 0.79 mmol) in $CHCl_3$ (10 mL). The reaction mixture was stirred at RT for 9 h under a nitrogen atmosphere, and then concentrated under vacuum to a volume of approximately 1 mL. Addition of diethyl ether (20 mL) to the residue produced a yellow precipitate, which was collected by filtration and washed with dichloromethane (2×2 mL) to obtain an insoluble yellow solid that was dried under vacuum to give **5** (283 mg, 55%).

Method b: A solution of H_2O_2 (73 μL, 0.72 mmol) was added to a suspension of **4b** (184 mg, 0.143 mmol) in $CHCl_3$ (10 mL). The reaction mixture was stirred at RT for 15 min to give a yellow solution, which was concentrated under vacuum to a volume of approximately 1 mL. Addition of diethyl ether (20 mL) to the residue produced a green precipitate, which was collected by filtration, washed with diethyl ether (2×5 mL) and dried under vacuum to give **5** (180 mg, 98%). Paramagnetism of **5** prevented characterization by NMR spectroscopy. HRMS (ESI): *m/z* calcd for $[C_{62}H_{57}Cl_2N_2OOsP_3]^+$: 1200.2670 $[M]^+$; found: 1200.2644; elemental analysis calcd (%) for $C_{62}H_{57}Cl_2N_2P_3BF_4OOs$: C 57.86, H 4.46, N 2.18; found: C 57.60, H 4.58, N 2.48.

Complex 6

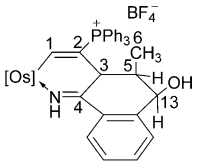

Method a: A solution of HI (400 μL, 2.5 mmol) was added to a solution of **1** (1.50 g, 1.25 mmol) and 2-cyanobenzaldehyde (328 mg, 2.50 mmol) in $CHCl_3$ (10 mL). The reaction mixture was stirred at RT for 5 h under a nitrogen atmosphere to give a yellow suspension. The yellow solid was collected by filtration, washed with diethyl ether (2×10 mL), washed with dichloromethane (2×2 mL), and dried under vacuum to give **6** (500 mg, 30%).

Method b: A solution of compound **7** (180 mg, 0.135 mmol) in $CHCl_3$ (15 mL) was stirred at RT under a H_2 atmosphere for 48 h to give a yellow solution, The solution was concentrated under vacuum to a volume of approximately 2 mL. Addition of diethyl ether (20 mL) to the solution gave a yellow precipitate, which was collected by filtration, washed with diethyl ether (2×5 mL), and dried under vacuum to give **6** (178 mg, 99%). Paramagnetism of **6** prevented characterization by NMR spectroscopy. HRMS (ESI): *m/z* calcd for $[C_{67}H_{58}Cl_2NOOsP_3]^+$: 1247.2718 $[M+H]^+$; found: 1247.2685; elemental analysis calcd (%) for $C_{67}H_{58}Cl_2NP_3BF_4OOs$: C 60.32, H 4.38, N 1.05; found: C 60.55, H 4.63, N 1.32.

Complex 7

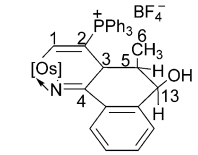

Method a: A solution of compound **6** (187 mg, 0.140 mmol) in $CHCl_3$ (15 mL) was stirred at RT under an O_2 atmosphere for 10 h to give a yellow solution, The solution was concentrated under vacuum to a volume of approximately 2 mL. Addition of diethyl ether (20 mL) to the solution gave a green precipitate, which was collected by filtration, washed with diethyl ether (2×5 mL), and dried under vacuum to give **7** (185 mg, 99%).

Method b: A solution of HNO_3 (10.3 μL, 0.152 mmol) was added to a suspension of **8** (200 mg, 0.150 mmol) in $CHCl_3$ (15 mL). The reaction mixture was stirred at RT for 10 h to give a yellow-green suspension. The green solid was collected by filtration, washed with diethyl ether (2×10 mL), then washed with dichloromethane (2×2 mL), and dried under vacuum to give **7** (100 mg, 50%). ^{1}H NMR (500.2 MHz, DMSO): $\delta = 12.6$ (d, J(P,H) = 30.0 Hz, 1H; C^1*H*), 9.2 (br, 1H; C^3*H*), 7.6–6.8 (m, 49H; Ph), 5.3 (br, 1H; O*H*), 4.2 (br, 1H; C^{13}*H*), 1.9 (br, 1H; C^5*H*), −0.6 ppm (br, 3H; C^6*H*); ^{13}C NMR (125.8 MHz, DMSO): $\delta = 180.5$ (br; C^1), 139.6 (s; C^{12}), 136.8 (d, J(P,C) = 8.3 Hz; C^4), 135.3–122.6 (m, Ph), 112.4 (d, J(P,C) = 75.9 Hz; C^2), 66.3 (s; C^{13}), 39.5 (s; C^5), 37.8 (d, J(P,C) = 21.3 Hz; C^3), 14.6 ppm (s; C^6); ^{31}P NMR (202.5 MHz, DMSO): $\delta = 17.0$ (s; C*P*Ph$_3$), −32.7 (d, J(P,P) = 385.2 Hz; Os*P*Ph$_3$), −35.1 ppm (d, J(P,P) = 385.2 Hz; Os*P*Ph$_3$); HRMS (ESI): *m/z* calcd for $[C_{67}H_{57}Cl_2NOOsP_3]^+$: 1246.2645 $[M]^+$; found: 1246.2624; elemental analysis calcd (%) for $C_{67}H_{57}Cl_2NP_3BF_4OOs$: C 60.37, H 4.31, N 1.05; found: C 60.41, H 4.51, N 1.31.

Complex 8

Method a: A mixture of **1** (505 mg, 0.42 mmol) and 2-cyanobenzaldehyde (110 mg, 0.84 mmol) in $CHCl_3$ (10 mL) was heated at reflux temperature for about 7 h in the presence of air to give a yellow solution. The solution was concentrated under vacuum to a volume of approximately 2 mL. Addition of diethyl ether (20 mL) to the solution gave a yellow precipitate, which was collected by filtration, washed with diethyl ether (2×5 mL), and dried under vacuum to give **8** (280 mg, 50%).

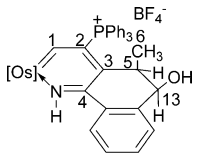

Method b: A solution of **6** (211 mg, 0.158 mmol) in $CHCl_3$ (15 mL) was heated at reflux temperature in the presence of air for 5 h to give a yellow solution. The solution was concentrated under vacuum to a volume of approximately 2 mL. Addition of diethyl ether (20 mL) to the solution gave a yellow precipitate, which was collected by filtration, washed with diethyl ether (2×5 mL), and dried under vacuum to give **8** (200 mg, 95%).

Method c: A solution of **7** (220 mg, 0.165 mmol) in $CHCl_3$ (15 mL) was heated at reflux temperature under an air atmosphere for 5 h to give a yellow solution. The solution was concentrated under vacuum to a volume of approximately 2 mL. Addition of diethyl ether (20 mL) to the solution gave a yellow precipitate, which was collected by filtration, washed with diethyl ether (2×5 mL), and dried under vacuum to give **8** (209 mg, 95%). ^{1}H NMR (500.2 MHz, DMSO): $\delta = 41.5$ (d, J(P,H) = 19.4 Hz, 1H; C^1*H*), 24.2 (s, 1H; N*H*), 7.9–6.9 (m, 49H; Ph), 5.8 (br, 1H; O*H*), 5.1 (br, 1H; C^{13}*H*), 4.0 (br, 1H; C^5*H*), 0.4 ppm (br, 3H; C^6*H*); ^{13}C NMR (128.5 MHz, DMSO): $\delta = 210.9$ (s; C^3), 207.7 (br; C^1), 150.7 (s; C^4), 136.5–123.5 (m; Ph), 122.5 (d, J(P,C) = 69.7 Hz; C^2), 82.9 (s; C^{13}), 35.4 (s; C^6), 33.1 ppm (s; C^5); ^{31}P NMR (202.5 MHz, DMSO): $\delta = 19.5$ (d, J(P,P) = 289.5 Hz; Os*P*Ph$_3$), 15.3 (s; C*P*Ph$_3$), −8.1 ppm (d, J(P,P) = 289.5 Hz; Os*P*Ph$_3$); HRMS (ESI): *m/z* calcd for $[C_{67}H_{57}Cl_2NOOsP_3]^+$: 1246.2645 $[M]^+$; found: 1246.2603; elemental analysis calcd (%) for $C_{67}H_{57}Cl_2NP_3BF_4OOs$: C 60.37, H 4.31, N 1.05; found: C 60.74, H 4.15, N 1.12.

Complex 9

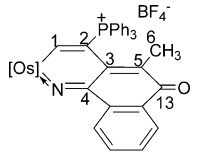

A solution of HNO_3 (103 μL, 1.52 mmol) was added to a suspension of **8** (507 mg, 0.380 mmol) in $CHCl_3$ (15 mL). The reaction mixture was stirred at RT for 6 h to give a yellow solution. The solution was concentrated under vacuum to a volume of approximately 1 mL. Addition of diethyl ether (20 mL) to the residue produced a yellow precipitate, which was collected by filtration, washed with diethyl ether (2×5 mL), and dried under vacuum to give **9** (490 mg, 97%). ^{1}H NMR (500.2 MHz, CD_2Cl_2): $\delta = 12.9$ (d, J(P,H) = 30.6 Hz, 1H; C^1*H*), 8.1–6.6 (m, 49H; Ph), 2.5 ppm (s, 3H; C^6*H*); ^{13}C NMR (125.8 MHz, CD_2Cl_2): $\delta = 195.9$ (br; C^1), 189.7 (s; C^4), 178.1 (s; C^{13}), 146.3 (s; C^5), 136.2–122.1 (m; Ph), 118.7 (d, J(P,C) = 19.3 Hz; C^3), 110.8 (d, J(P,C) = 76.8 Hz; C^2), 19.9 ppm (s; C^6); ^{31}P NMR (202.5 MHz, CD_2Cl_2): $\delta = 27.8$ (s; C*P*Ph$_3$), −24.9 ppm (s; Os*P*Ph$_3$); HRMS (ESI): *m/z* calcd for $[C_{67}H_{53}Cl_2NOOsP_3]^+$: 1242.2326 $[M]^+$; found: 1242.2312; elemental analysis calcd (%) for $C_{67}H_{53}Cl_2NOP_3BF_4Os$: C 60.55, H 4.02, N 1.05; found: C 60.54, H 4.06, N 1.43.

Complex 10

A solution of HCl (65 μL, 0.75 mmol) was added to a solution of **9** (200 mg, 0.15 mmol) in $CHCl_3$ (15 mL). The reaction mixture was heated at reflux temperature for about 7.5 h to give a purple solution. The solution was concentrated under vacuum to a volume approximately of 1 mL. Addition of diethyl ether (20 mL) to the residue produced a purple precipitate, which was collected by filtration, washed with diethyl ether (2×5 mL), and dried under vacuum

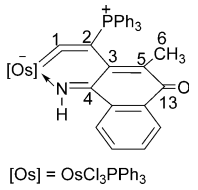

[Os] = $OsCl_3PPh_3$

to give **10** (107 mg, 70%). ^{1}H NMR (400.1 MHz, $CDCl_3$): $\delta = 12.6$ (s, 1H; N*H*), 8.0–7.1 (m, 34H; Ph), 1.3 ppm (s, 3H; C^6H); ^{13}C NMR (100.6 MHz, $CDCl_3$): $\delta = 281.2$ (br; C^1), 180.5 (s; C^{13}), 157.2 (s; C^4), 141.1 (s; C^5), 135.1–123.1 (m; Ph), 130.2 (s; C^3), 122.4 (d, J(P,C) = 90.8 Hz; C^2), 16.6 ppm (s; C^6); ^{31}P NMR (162 MHz, $CDCl_3$): $\delta = 5.8$ (s; $CPPh_3$), −4.9 ppm (s; $OsPPh_3$); HRMS (ESI): *m/z* calcd for $[C_{49}H_{38}Cl_3NOOsP_2 + Na]^+$: 1038.1007 [$M$ + Na]$^+$; found: 1038.0977; elemental analysis calcd (%) for $C_{49}H_{38}Cl_3NOP_2Os$: C 57.96, H 3.77, N 1.38; found: C 57.74, H 3.65, N 1.52.

Complex 11

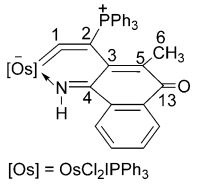

[Os] = $OsCl_2IPPh_3$

A solution of HI (120 μL, 0.75 mmol) was added to a solution of **9** (200 mg, 0.15 mmol) in $CHCl_3$ (15 mL). The reaction mixture was heated at reflux temperature for about 2 h to give a purple solution. The solution was concentrated under vacuum to a volume of approximately 1 mL. Addition of diethyl ether (20 mL) to the residue produced a purple precipitate, which was collected by filtration, washed with diethyl ether (2×5 mL), and dried under vacuum to give **11** (66 mg, 40%). ^{1}H NMR (400.1 MHz, CD_2Cl_2): $\delta = 12.3$ (s, 1H; N*H*), 8.0–6.9 (m, 34H; Ph), 1.2 ppm (s, 3H; C^6H); ^{13}C NMR: poor solubility of **11** prevented characterization by ^{13}C NMR spectroscopy; ^{31}P NMR (162.0 MHz, CD_2Cl_2): $\delta = 5.9$ (s; $CPPh_3$), −5.8 ppm (s; $OsPPh_3$); HRMS (ESI): *m/z* calcd for $[C_{49}H_{38}Cl_2NOOsP_2]^+$: 980.1420 [$M$−I]$^+$; found: 980.1393; elemental analysis calcd (%) for $C_{49}H_{38}Cl_2INOP_2Os$: C 53.17, H 3.46, N 1.27; found: C 52.80, H 3.23, N 1.49.

Crystallographic details

Single-crystal X-ray diffraction data were collected with an Oxford Gemini S Ultra or a Rigaku R-AXIS SPIDER IP CCD area detector by using graphite-monochromated $Mo_{K\alpha}$ radiation ($\lambda = 0.71073$ Å). Multiscan absorption corrections (SADABS) were applied. All structures were solved by direct methods, expanded by difference Fourier syntheses, and refined via a full-matrix least-squares method on F^2 by using the Bruker SHELXTL-97 program package. Non-hydrogen atoms were refined anisotropically unless otherwise stated. Hydrogen atoms were introduced at their geometric positions and refined as riding atoms unless otherwise stated. CCDC 970569 (**2a**), 970570 (**3a**), 970567 (**4a**), 1428315 (**4b**), 1428316 (**5**), 1428317 (**6**), 1428318 (**7**), 1428319 (**8**), 1428320 (**9**), 1428321 (**10**), and 1428322 (**11**) contain the supplementary crystallographic data for this paper. These data can be obtained free of charge from The Cambridge Crystallographic Data Centre via www.ccdc.cam.ac.uk/data_request/cif.

Acknowledgements

This research was supported by the NSFC (nos. 21272193, 21332002, 21490573, and 21572185), the program for Changjiang Scholars and Innovative Research Team in University, and the Fundamental Research Funds for the Central Universities (no. 20720150046).

Keywords: azavinylidenes · cycloaddition · isometallapyridiniums · metallacycles · vinylidenes

[1] For selected reviews of vinylidene chemistry, see: a) A. Ishii, N. Nakata in, *Topics in Organometallic Chemistry, Vol. 43: Hydrofunctionalization* (Eds.: V. P. Ananikov, M. Tanaka), Springer, Berlin Heidelberg, **2013**, pp. 21–50; b) J. M. Lynam, *Chem. Eur. J.* **2010**, *16*, 8238–8247; c) J. A. Varela, C. González-Rodríguez, S. G. Rubín, L. Castedo, C. Saá, *Pure Appl. Chem.* **2008**, *80*, 1167–1177; d) B. M. Trost, A. McClory, *Chem. Asian J.* **2008**, *3*, 164–194; e) C. Bruneau, P. H. Dixneuf, *Metal Vinylidenes & Allenylidenes in Catalysis from Reactivity to Applications in Synthesis*, Wiley-VCH, Weinheim, **2008**; f) J. A. Varela, C. Saá, *Chem. Eur. J.* **2006**, *12*, 6450–6456; g) C. Bruneau, P. H. Dixneuf, *Angew. Chem. Int. Ed.* **2006**, *45*, 2176–2203; *Angew. Chem.* **2006**, *118*, 2232–2260; h) Y. Wakatsuki, *J. Organomet. Chem.* **2004**, *689*, 4092–4109; i) D. A. Valyaev, O. V. Semeikin, N. A. Ustynyuk, *Coord. Chem. Rev.* **2004**, *248*, 1679–1692; j) C. Bruneau, P. H. Dixneuf, *Acc. Chem. Res.* **1999**, *32*, 311–323; k) M. I. Bruce, *Chem. Rev.* **1991**, *91*, 197–257.

[2] R. B. King, M. S. Saran, *J. Chem. Soc. Chem. Commun.* **1972**, 1053–1054.

[3] Recent examples of vinylidene complexes as key intermediates: a) J. V. Obligacion, J. M. Neely, A. N. Yazdani, I. Pappas, P. J. Chirik, *J. Am. Chem. Soc.* **2015**, *137*, 5855–5858; b) P. Morán-Poladura, E. Rubio, J. M. González, *Angew. Chem. Int. Ed.* **2015**, *54*, 3052–3055; *Angew. Chem.* **2015**, *127*, 3095–3098; c) S. Hori, M. Murai, K. Takai, *J. Am. Chem. Soc.* **2015**, *137*, 1452–1457; d) J. Bucher, T. Stößer, M. Rudolph, F. Rominger, A. S. K. Hashmi, *Angew. Chem. Int. Ed.* **2015**, *54*, 1666–1670; *Angew. Chem.* **2015**, *127*, 1686–1690; e) J. Bucher, T. Wurm, K. S. Nalivela, M. Rudolph, F. Rominger, A. S. K. Hashmi, *Angew. Chem. Int. Ed.* **2014**, *53*, 3854–3858; *Angew. Chem.* **2014**, *126*, 3934–3939; f) M. P. Boone, D. W. Stephan, *Organometallics* **2014**, *33*, 387–393; g) I. Kim, C. Lee, *Angew. Chem. Int. Ed.* **2013**, *52*, 10023–10026; *Angew. Chem.* **2013**, *125*, 10207–10210; h) D. G. Johnson, J. M. Lynam, N. S. Mistry, J. M. Slattery, R. J. Thatcher, A. C. Whitwood, *J. Am. Chem. Soc.* **2013**, *135*, 2222–2234; i) Y. Mutoh, Y. Kimura, Y. Ikeda, N. Tsuchida, K. Takano, Y. Ishii, *Organometallics* **2012**, *31*, 5150–5158; j) X. Kang, N. B. Zuckerman, J. P. Konopelski, S. Chen, *J. Am. Chem. Soc.* **2012**, *134*, 1412–1415; k) A. S. K. Hashmi, M. Wieteck, I. Braun, M. Rudolph, F. Rominger, *Angew. Chem. Int. Ed.* **2012**, *51*, 10633–10637; *Angew. Chem.* **2012**, *124*, 10785–10789; l) J. H. Bowie, M. I. Bruce, M. A. Buntine, A. S. Gentleman, D. C. Graham, P. J. Low, G. F. Metha, C. Mitchell, C. R. Parker, B. W. Skelton, A. H. White, *Organometallics* **2012**, *31*, 5262–5273; m) M. L. Buil, M. A. Esteruelas, K. Garcés, E. Oñate, *J. Am. Chem. Soc.* **2011**, *133*, 2250–2263; n) A. Collado, M. A. Esteruelas, F. López, J. L. Mascareñas, E. Oñate, B. Trillo, *Organometallics* **2010**, *29*, 4966–4974.

[4] Recent examples of vinylidene complexes as active substrates: a) G. Albertin, S. Antoniutti, M. Bortoluzzi, A. Botter, J. Castro, *Dalton Trans.* **2015**, *44*, 3439–3446; b) M. Jiménez-Tenorio, M. C. Puerta, P. Valerga, M. A. Ortuño, G. Ujaque, A. Lledós, *Organometallics* **2014**, *33*, 2549–2560; c) Q. Zhao, X.-Y. Cao, T. B. Wen, H. Xia, *Chem. Asian J.* **2013**, *8*, 269–275; d) E. A. Ivanova Shor, V. A. Nasluzov, A. M. Shor, A. B. Antonova, N. Rösch, *J. Organomet. Chem.* **2011**, *696*, 3445–3453; e) Y. Mutoh, K. Imai, Y. Kimura, Y. Ikeda, Y. Ishii, *Organometallics* **2011**, *30*, 204–207; f) M. Batuecas, L. Escalante, M. A. Esteruelas, C. García-Yebra, E. Oñate, C. Saá, *Angew. Chem. Int. Ed.* **2011**, *50*, 9712–9715; *Angew. Chem.* **2011**, *123*, 9886–9889.

[5] a) P. Barrio, M. A. Esteruelas, E. Oñate, *J. Am. Chem. Soc.* **2004**, *126*, 1946–1947; b) Q. Zhao, L. Gong, C. Xu, J. Zhu, X. He, H. Xia, Q. Zhao, L. Gong, C. Xu, J. Zhu, X. He, H. Xia, *Angew. Chem. Int. Ed.* **2011**, *50*, 1354–1358; *Angew. Chem.* **2011**, *123*, 1390–1394; c) Q. Zhao, J. Zhu, Z.-A. Huang, X.-Y. Cao, H. Xia, *Chem. Eur. J.* **2012**, *18*, 11597–11603.

[6] T. Wang, J. Zhu, F. Han, C. Zhou, H. Chen, H. Zhang, H. Xia, *Angew. Chem. Int. Ed.* **2013**, *52*, 13361–13364; *Angew. Chem.* **2013**, *125*, 13603–13606.

[7] M. J. Ferreira, A. M. Martins, *Coord. Chem. Rev.* **2006**, *250*, 118–132.

[8] Recent examples of azavinylidene–metal complexes, see: a) J.-S. Huang, K.-M. Wong, S. L.-F. Chan, K. C.-H. Tso, T. Jiang, C.-M. Che, *Chem. Asian J.* **2014**, *9*, 338–350; b) S. K. Podiyanachari, R. Fröhlich, C. G. Daniliuc, J. L. Petersen, C. Mück-Lichtenfeld, G. Kehr, G. Erker, *Angew. Chem. Int. Ed.* **2012**, *51*, 8830–8833; *Angew. Chem.* **2012**, *124*, 8960–8963; c) E. Lu, Q.

Zhou, Y. Li, J. Chu, Y. Chen, X. Leng, J. Sun, *Chem. Commun.* **2012**, *48*, 3403 – 3405; d) J. Ugolotti, G. Kehr, R. Fröhlich, S. Grimme, G. Erker, *Chem. Commun.* **2009**, 6572 – 6573; e) A. R. Cowley, J. R. Dilworth, A. K. Nairn, A. J. Robbie, *Dalton Trans.* **2005**, 680 – 693; f) M. I. Bruce, M. A. Buntine, K. Costuas, B. G. Ellis, J.-F. Halet, P. J. Low, B. W. Skelton, A. H. White, *J. Organomet. Chem.* **2004**, *689*, 3308 – 3326; g) M. F. C. Guedes da Silva, J. J. R. Fraústo da Silva, A. J. L. Pombeiro, *Inorg. Chem.* **2002**, *41*, 219 – 228; h) S. M. P. R. M. Cunha, M. F. C. Guedes da Silva, A. J. L. Pombeiro, *J. Chem. Soc. Dalton Trans.* **2002**, 1791 – 1799; i) R. Castarlenas, M. A. Esteruelas, E. Oñate, *Organometallics* **2001**, *20*, 3283 – 3292; j) R. Castarlenas, M. A. Esteruelas, Y. Jean, A. Lledós, E. Oñate, J. Tomàs, *Eur. J. Inorg. Chem.* **2001**, *2001*, 2871 – 2883; k) R. Castarlenas, M. A. Esteruelas, E. Gutiérrez-Puebla, E. Oñate, *Organometallics* **2001**, *20*, 1545 – 1554; l) Y. Tanabe, H. Seino, Y. Ishii, M. Hidai, *J. Am. Chem. Soc.* **2000**, *122*, 1690 – 1699; m) R. Castarlenas, M. A. Esteruelas, E. Gutiérrez-Puebla, Y. Jean, A. Lledós, M. Martín, E. Oñate, J. Tomàs, *Organometallics* **2000**, *19*, 3100 – 3108; n) S. N. Brown, *Inorg. Chem.* **2000**, *39*, 378 – 381.

[9] a) T. R. Mohs, Y. Du, B. Plashko, E. A. Maatta, *Chem. Commun.* **1997**, 1707 – 1708; b) E. A. Maatta, Y. Du, *J. Am. Chem. Soc.* **1988**, *110*, 8249 – 8250.

[10] a) Q. X. Dai, H. Seino, Y. Mizobe, *Organometallics* **2012**, *31*, 4933 – 4936; b) N. J. Vogeley, J. L. Templeton, *Polyhedron* **2004**, *23*, 311 – 321; c) A. C. Hillier, T. Fox, H. W. Schmalle, H. Berke, *J. Organomet. Chem.* **2003**, *669*, 14 – 24; d) W.-Y. Yeh, C.-S. Ting, S.-M. Peng, G.-H. Lee, *Organometallics* **1995**, *14*, 1417 – 1422; e) S. G. Feng, P. S. White, J. L. Templeton, *J. Am. Chem. Soc.* **1994**, *116*, 8613 – 8620; f) S. G. Feng, J. L. Templeton, *Organometallics* **1992**, *11*, 1295 – 1303; g) J. D. Debad, P. Legzdins, R. J. Batchelor, F. W. B. Einstein, *Organometallics* **1992**, *11*, 6 – 8; h) S. G. Feng, J. L. Templeton, *J. Am. Chem. Soc.* **1989**, *111*, 6477 – 6478; i) L. F. Rhodes, L. M. Venanzi, *Inorg. Chem.* **1987**, *26*, 2692 – 2695.

[11] B. Liu, H. Wang, H. Xie, B. Zeng, J. Chen, J. Tao, T. B. Wen, Z. Cao, H. Xia, *Angew. Chem. Int. Ed.* **2009**, *48*, 5430 – 5434; *Angew. Chem.* **2009**, *121*, 5538 – 5542.

[12] J. Chen, C. Zhang, T. Xie, T. B. Wen, H. Zhang, H. Xia, *Organometallics* **2013**, *32*, 3993 – 4001.

[13] B. Liu, Q. Zhao, H. Wang, J. Chen, X. Cao, Z. Cao, H. Xia, *Chin. J. Chem.* **2012**, *30*, 2158 – 2168.

[14] For recent reviews on the chemistry of metalla-aromatics, see: a) G. Jia, *Organometallics* **2013**, *32*, 6852 – 6866; b) J. Chen, G. Jia, *Coord. Chem. Rev.* **2013**, *257*, 2491 – 2521; c) C. Zhu, X. Cao, H. Xia, *Chin. J. Org. Chem.* **2013**, *33*, 657 – 662; d) M. Paneque, M. L. Poveda, N. Rendon, *Eur. J. Inorg. Chem.* **2011**, 19 – 33; e) G. Jia, *Coord. Chem. Rev.* **2007**, *251*, 2167 – 2187; f) J. R. Bleeke, *Acc. Chem. Res.* **2007**, *40*, 1035 – 1047; g) L. J. Wright, *Dalton Trans.* **2006**, 1821 – 1827; h) C. W. Landorf, M. M. Haley, *Angew. Chem. Int. Ed.* **2006**, *45*, 3914 – 3936; *Angew. Chem.* **2006**, *118*, 4018 – 4040; i) G. Jia, *Acc. Chem. Res.* **2004**, *37*, 479 – 486; j) J. R. Bleeke, *Chem. Rev.* **2001**, *101*, 1205 – 1227.

[15] Based on a search of the Cambridge Structural Database. The latest update to the database at the time of writing was February 2015.

[16] For examples of azavinylidene–osmium complexes, see: a) J. L. Koch, P. A. Shapley, *Organometallics* **1999**, *18*, 814 – 816; b) H. Werner, T. Daniel, M. Mueller, N. Mahr, *J. Organomet. Chem.* **1996**, *512*, 197 – 205; c) H. Werner, W. Knaup, M. Dziallas, *Angew. Chem. Int. Ed. Engl.* **1987**, *26*, 248 – 250; *Angew. Chem.* **1987**, *99*, 277 – 278.

[17] T. Wang, H. Zhang, F. Han, R. Lin, Z. Lin, H. Xia, *Angew. Chem. Int. Ed.* **2012**, *51*, 9838 – 9841; *Angew. Chem.* **2012**, *124*, 9976 – 9979.

[18] R. Lin, J. Zhao, H. Chen, H. Zhang, H. Xia, *Chem. Asian J.* **2012**, *7*, 1915 – 1924.

[19] a) R. Castro-Rodrigo, M. A. Esteruelas, A. M. López, E. Oñate, *Organometallics* **2008**, *27*, 3547 – 3555; b) T. Bolaño, R. Castarlenas, M. A. Esteruelas, E. Oñate, *Organometallics* **2007**, *26*, 2037 – 2041; c) T. Bolaño, R. Castarlenas, M. A. Esteruelas, F. J. Modrego, E. Oñate, *J. Am. Chem. Soc.* **2005**, *127*, 11184 – 11195.

[20] M. A. Esteruelas, Y. A. Hernández, A. M. López, M. Oliván, E. Oñate, *Organometallics* **2005**, *24*, 5989 – 6000, and references therein.

[21] P. v. R. Schleyer, F. Pühlhofer, *Org. Lett.* **2002**, *4*, 2873 – 2876.

[22] W. J. Hehre, R. Ditchfield, L. Radom, J. A. Pople, *J. Am. Chem. Soc.* **1970**, *92*, 4796 – 4801.

[23] Detailed results of the DFT calculations are provided in the Supporting Information.

[24] K. Kaleta, M. Ruhmann, O. Theilmann, T. Beweries, S. Roy, P. Arndt, A. Villinger, E. D. Jemmis, A. Schulz, U. Rosenthal, *J. Am. Chem. Soc.* **2011**, *133*, 5463 – 5473.

Received: November 17, 2015
Published online on February 26, 2016